Version of Record: https://www.sciencedirect.com/science/article/pii/S0022407319303310
Manuscript_b41b5be188cb0801c2d914c22fc97b06

Using multi-wavelength Mie-Raman Lidar to measure low-level cloud properties

Jia Su* and M. Patrick McCormick

Center for Atmospheric Sciences, Department of Atmospheric and Planetary Sciences, Hampton University, Hampton, Virginia 23668, USA

Corresponding author: jia.su@hamptonu.edu

Highlights:

- Low-level cloud properties are obtained by combining Mie, vibrational and rotational Raman lidars.
- Relationship between cloud lidar ratio and temperature difference of cloud base and top, relationship between cloud lidar ratio and optical depth and relation of cloud optical depth and temperature difference of cloud base and top are discussed and summarized.
- These quantitative analyses of simultaneous measurements can improve the understanding of low-level cloud effects of radiative transfer.

Keywords: Lidar, Cloud, Raman

Abstract

Because clouds can result in a warming or a cooling effect according to their characteristics and altitudes, they have a significant influence on the climate system and a better understanding of cloud properties can improve weather forecasts and global climate models. Mie and Raman lidars have been proven to be very useful remote sensing tools to measure low-level cloud properties and locations. In this paper, low-level cloud boundary (top and base), temperature, extinction coefficients, optical depth (OD) and lidar ratio are obtained by combining Mie, rotational Raman (RR) and vibrational Raman (VR) techniques. These results of low-level cloud properties measured by the Hampton University (HU) Mie-Rotational-Vibrational Raman Lidar describe the relation between cloud lidar ratio and temperature, the relation between cloud lidar ratio and OD and the relation between cloud OD and temperature. The relationship between cloud OD and cloud lidar ratios is relatively strong, while the relationship between cloud lidar ratios and temperature difference of cloud base and top (DCBT) and between DCBT and cloud OD is relatively weak. These quantitative analyses of simultaneous measurements can improve the understanding of low-level cloud effects of radiative transfer.

1 Introduction

The research of clouds is very critical Accurate measurements of cloud optical properties are important for improving our understanding of cloud physics, cloud dynamics, and cloud parameterizations in global climate models (Albrecht et al., 1979; Sinkevich et al., 2005) and for understanding and predicting the climate system and earth's radiation budget (Solomon et al. 2007).Obtaining cloud optical properties requires collecting and analyzing long-term and

extensive observations with in-situ and remote-sensing measurements (Stokes and Schwartz 1994; Rossow and Schiffer 1999). Space-borne passive remote sensing (e.g., performed by the Moderate Resolution Imaging Spectroradiometer, MODIS), can observe cloud amount and top height on a global scale (Platnick et al., 2003). However, their retrieval accuracy suffers from various limitations. Moreover, the properties of low-level clouds are difficult to detect by passive satellite sensors with visible and near-infrared channels. Space-borne, active remote sensors, such as Cloud-Aerosol Lidar Pathfinder Satellite Observations (CALIPSO) and CloudSat, can obtain cloud vertical structure such as cloud boundary, cloud extinction, cloud backscatter, and water phase, however, the limited temporal resolution irenders investigation of the diurnal cycle of clouds over specific regions impossible (Winker et al., 2003).

Mie-Raman Lidars are very useful remote sensing tools to accurately obtain knowledge about low-level cloud optical properties. Cloud top and base can be retrieved from Mie backscatter and atmospheric temperature can be measured using rotational Raman lidars (Cooney, 1972; Arshinov et al., 1983). Moreover, the capabilities of rotational Raman technique extend to the measurement of cloud temperature. When a cloud is not optically thick and its backscatter ratio is smaller than 45, cloud temperature can be measured using RR lidar with the multi-cavity polychromator (Behrendt et al., 2000). Su et. al designed a technique to calculate the leaking coefficients of the residual elastic-signal on RR channels and can obtain thick cloud temperature using the leaking coefficients (Su et al., 2013). Cloud extinction and OD can be independently obtained from a nitrogen vibrational Raman signal without assuming lidar ratios (Ansmann et al., 1990). Cloud backscattering and lidar ratio can be obtained using combing Mie signal and vibrational Raman signal. In this paper, cloud temperature, cloud lidar ratios, cloud extinction coefficients, cloud OD, and cloud boundary (top and base height) are retrieved using Mie, RR and vibrational Raman, wavelet, and transmittance ratio constrained techniques respectively. These quantitative analyses of simultaneous measurements can improve our understanding of low-level cloud effects on radiative transfer.

2 Materials and Methods

2.1 Wavelet method to obtain cloud boundary

The wavelet covariance transform (WCT) provides an objective method to detect the step change in a signal (Davis et al., 2000); therefore, we used it to detect the rapid change in lidar elastic signal ($X(z)$). The first step is to calculate the following covariance transform

$$W_f(a,b) = \frac{1}{a}\int_{z_b}^{z_t} X(z)h(\frac{z-b}{a})dz \tag{1}$$

This transform is the convolution of $X(z)$ with the Haar function defined by (Brooks, 2003; Compton et al., 2013)

$$h\left(\frac{z-b}{a}\right) = \begin{cases} +1 : b - \frac{a}{2} \le z \le b \\ -1 : b \le z \le b + \frac{a}{2} \\ 0 : elsewhere \end{cases} \tag{2}$$

In both (1) and (2), z is altitude and a and b are parameters that characterize the dilation and translation of the function, respectively. In addition, z_b and z_t in (2) are the bottom and top altitudes in the lidar profile, respectively. The maximum value of W_f identifies a step-change in $X(z)$; therefore, the value of z at which this occurs is taken to be the cloud boundary height (Paleti et al., 2013; Davis, 2000) when the atmosphere is clear.

2.2 Vibrational Raman method to obtain cloud extinction and cloud OD

The cloud extinction coefficients can be obtained using vibrational technique showed in the equation below (Ansmann et al., 1990):

$$a_{a,e}(z) = \frac{\frac{d}{d} In\left[\frac{N(z)}{X_r(z)}\right] - a_{m,e}(z) - a_{m,r}(z)}{1+\left(\frac{\lambda_e}{\lambda_r}\right)^k} \tag{3}$$

Where $N(z)$ is the atmospheric number density of the Raman scattering, k is the Angstrom exponent; β and α are the backscattering and extinction coefficients; the subscripts e and r represent the wavelength of elastic backscattering and the N_2 Raman scattering, and a and m represent aerosol and molecular scatterings; X is the range-corrected lidar return signal; z is the altitude; λ is wavelength.

Cloud OD can be obtained using N_2 VR signals and written as:

$$OD = \frac{In\left[\frac{X_r(z_{top})}{X_r(z_{base})} \times \frac{N(z_{base})}{N(z_{top})}\right]}{-2} - \sum_{z=base}^{z=top} T_m(z)dz \tag{4}$$

Where the subscripts of r, m, top and $base$ refer to Raman, molecular, cloud top and base; X is the lidar signal; z is altitude; OD is optical depth; T is molecular extinction; dz is lidar range resolution.

2.3 Rotational Raman method to obtain cloud temperature

Cloud temperature can be derived from two rotational Raman signals and written as (Su et al., 2013):

$$T(z) = \frac{a}{In\left(\frac{X^L_{r1}(z,\lambda_{r1}) - k_1 X_e(z,\lambda_e)}{X^L_{r2}(z,\lambda_{r2}) - k_2 X_e(z,\lambda_e)}\right) + b} \tag{5}$$

where the subscripts of X_e, X^L_{r1} and X^L_{r2} refer to one elastic and two RR backscattering signals; λ is wavelength; z is altitude; T is temperature; a and b are calibrated coefficients obtained using a balloon-sounding temperature profile; k_1 and k_2 are two RR channels' transmission for elastic backscatter signals from HU lidar elastic channel.

2.4 Transmittance ratio constrained retrieval technique to obtain cloud lidar ratios

Su et al., 2012 advanced a new lidar retrieval technique that uses the transmittance ratio as a constraint to determine an average lidar ratio of clouds. The cloud transmittance ratio is obtained directly from two adjacent elastic lidar backscatter signals. This technique can be

applied to cirrus measurements where neither the molecular scattering dominates signals above or below the cloud layer nor cloud-free reference profiles are available.

The cloud transmittance ratio (R_T) can be obtained from Equations (6).

$$R_T = \frac{X_r(t_1, z_{base}) X_r(t_2, z_{top})}{X_r(t_1, z_{top}) X_r(t_2, z_{base})} \tag{6}$$

$$P(S_c) = \left| R_T(S_c) - R_T \right| \tag{7}$$

Calculating trial values of S_c (from 1 to 70 sr with 1 sr increment) applied to Fernald solution of the lidar equation produces the cloud transmittance ratio $R_T(S_c)$. Using the performance function $P(S_c)$ determines S_c when $P(S_c)$ is minimized.

3 Equipment

The existing HU lidar system shown in Figure 1 (Su et al., 2010) currently consists of a zenith-viewing Nd:YAG laser that operates at three fixed laser wavelengths (1064, 532, and 355 nm), a 48-inch non-coaxial Cassegrain telescope receiver with 1~4 mrad field-of-view, a wavelength separation system using beam splitters and interference filters, detecting system including photomultiplier tube (PMT) and avalanche photodiode (APD), and a Licel optical transient recorder data reduction system. The lidar can be configured to measure elastic backscattering from aerosols and clouds at the three laser output wavelengths, and at the same time measure Raman scattering excited by the 355-nm laser third harmonic output with high resolution (7.5 m). The detected return signals are between the ranges of 1 to 30 km. Two lidar elastic signals (355 nm and 532 nm) and three Raman backscattered signals (353.35 nm, 354.2 nm and 386 nm) are received by five PMTs, while one lidar elastic signal (1064 nm) is received by an APD. This receiver arrangement provides the ability for HU lidar to measure aerosol backscatter and extinction coefficients from the elastic signals, and temperature, lidar ratios and OD from the rotational and vibrational Raman signals, respectively, with a vertical range that extends from the near-surface to the top of the troposphere depending on atmospheric conditions. Fig.1 shows the structure and filter system of HU lidar.

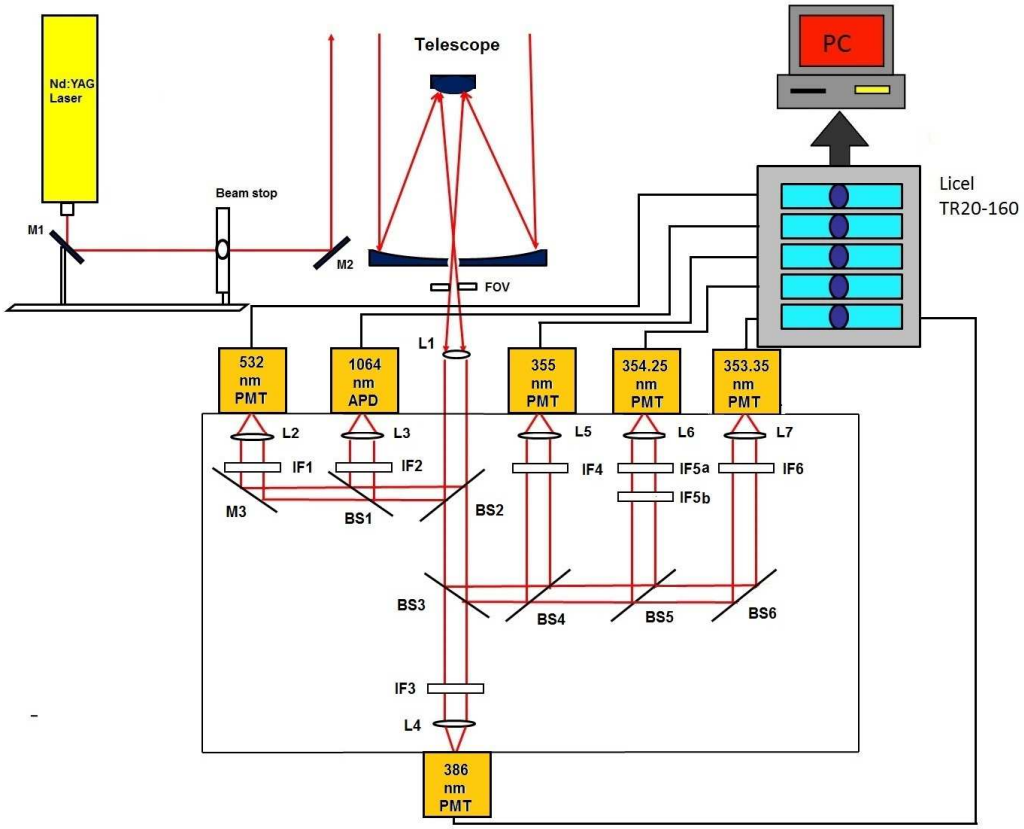

Fig.1 HU lidar system (L-lens, M-mirror, BS-beamsplitter, IF-interference filter, FOV-field of view, PMT-Photomultiplier tube, APD-Avalanche Photodetector)

4 Results

We present two low-level cloud cases measured by HU lidar to demonstrate the technique described above. Fig. 2(a) and (3)a respectively show lidar elastic backscatter signals with 2-min average at 1064 nm obtained by HU lidar from 19:30 to 22:30 on 01 November, 2010 and from 22:00 on 23 August, 2011 to 04:00 on 24 August, 2011 (local time). For the two cases, the clouds occurred at heights between 4.5-5.5 km in Fig. 2(a) and between 1.9-2.4 km in Fig. 3(a). Clouds in Fig. 2(a) maintained a few hours life-time from 19:30 to 22:30 on 01 November 2010 with stable depths. However, the clouds in Fig. 3(a) descend to the height between 1.7-2.1 km from 00:30 to 04:00 on 24 August 2011. Fig. 2(b) and 3(b) present the HU lidar cloud extinction coefficients (355 nm) retrieved using vibrational Raman technique for the same time periods. Presented in Fig. 2(c) and 3(c) are the temporal variation of HU lidar temperature retrieved using rotational Raman technique for the same time periods. Fig. 2(d) and 3(d) show the height of cloud top and base retrieved using wavelet technique from HU lidar 1064 nm range-corrected signals for the same time periods. Fig 2(e) and 3(e) show 355 nm cloud OD variation retrieved using vibrational Raman technique for the same time periods. Fig. 2(f) and 3(f) show the results of cloud lidar ratios retrieved using transmittance ratio constrained retrieval technique for the same time periods. Fig.4 (a), (b) and (c) show scatter plots of cloud OD as a function of cloud lidar ratios, cloud lidar ratios as a function of DCBT and cloud OD as a

function of DCBT for the two cases. To avoid retrieval errors of cloud properties using low SNR signals caused by strong clouds, all retrieved cloud results are removed in Fig.4 when cloud OD is more than 1.5. From Fig.4, it is found that the lidar ratio of low-level clouds is between 10 sr to 40 sr, DCBT is between 0.2 K and 1 K, and OD of low-level clouds is more than 0.4 in Hampton VA. The values of the correlation coefficient (R^2) shown in Fig.4 (a), (b) and (c) are 0.52, 0.21 and 0.1, respectively. These results show the relationship between cloud OD and cloud lidar ratios is relatively strong, while the relationship between cloud lidar ratios and DCBT and between DCBT and cloud OD is relatively weak.

5 Conclusions

This work combined Mie-Raman lidar to measure low-level cloud optical properties to explore the relationship between DCBT, OD and lidar ratios. Low-level cloud temperature, boundary, lidar ratios, extinction and OD are obtained using the wavelet, rotational Raman, vibrational Raman and transmittance ratio constrained retrieval techniques. A nocturnal result of low-level cloud optical properties observed by the HU Lidar shows cloud temperature base and top, and cloud OD. The relationship between cloud OD and cloud lidar ratios, and between cloud lidar ratios and cloud temperature, are relatively strong, while the relationship between cloud temperature and cloud OD is relatively weak. We will continue studying this outcome in the future.

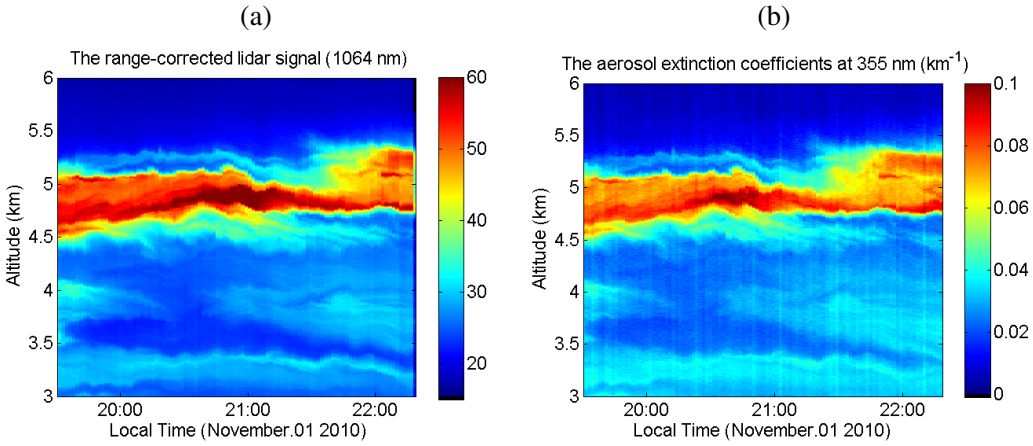

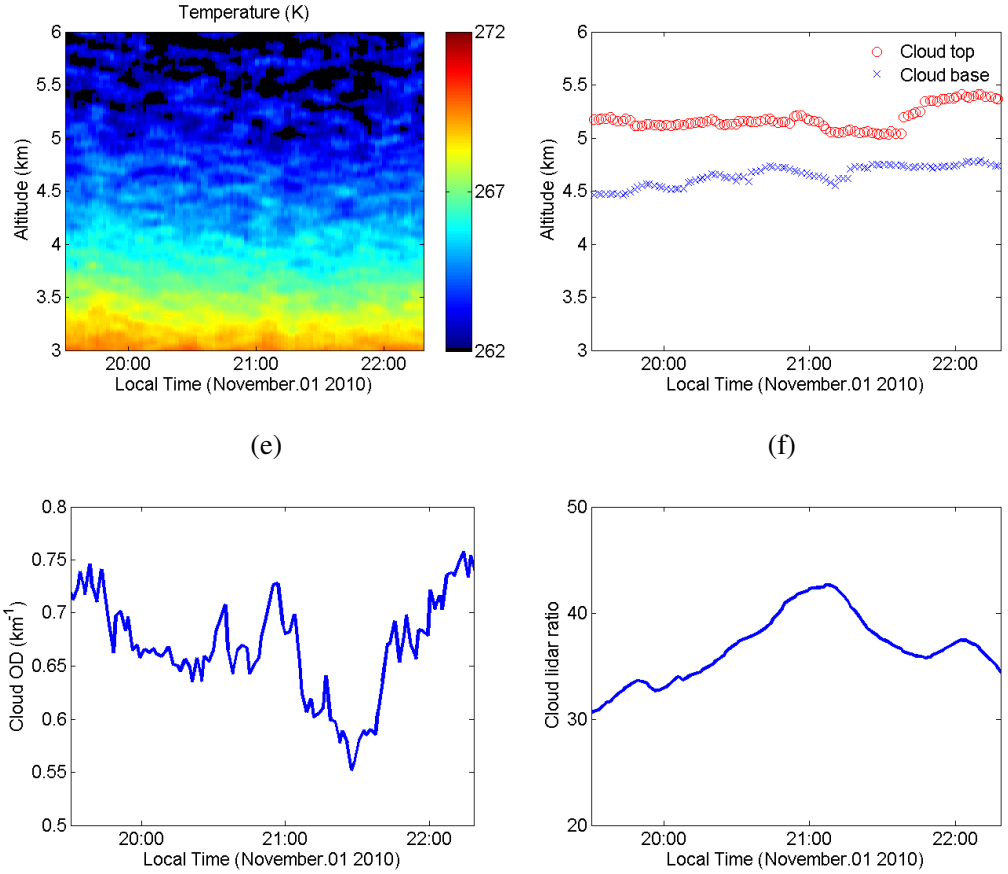

(e) (f)

Fig.2 (a) Range-corrected signals (1064 nm) (b) Aerosol and cloud extinction coefficients; (c) Temperature; (d) Height of cloud top and base; (e) cloud OD; (f) Cloud lidar ratios retrieved by HU lidar from 19:30 to 22:30 on 01 November, 2010 (local time).

(a) (b)

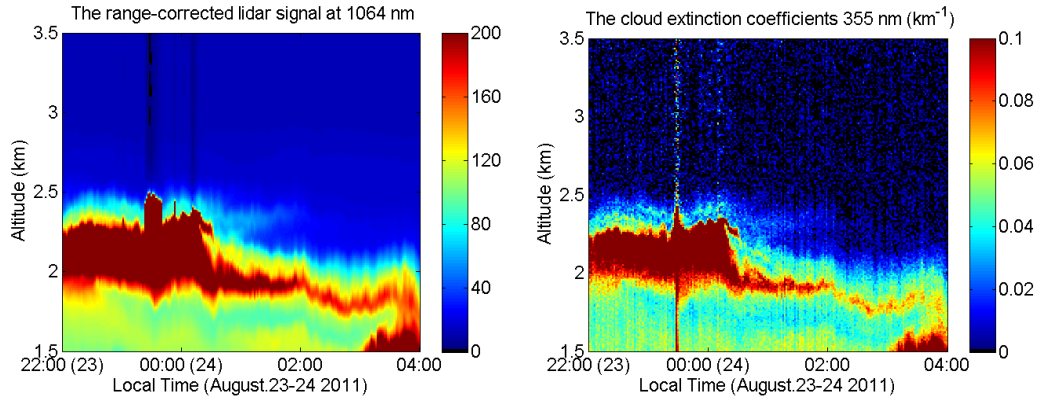

(c) (d)

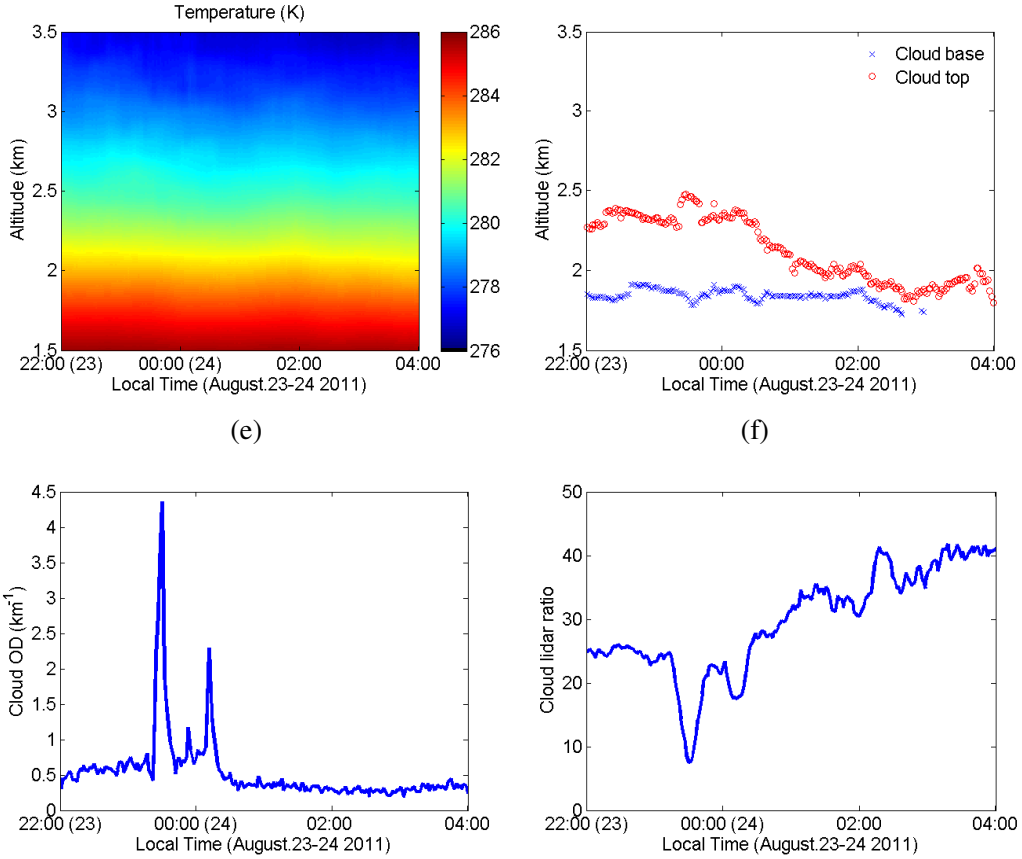

Fig.3 (a) Range-corrected signals (1064 nm) (b) Aerosol and cloud extinction coefficients; (c) Temperature; (d) Height of cloud top and base; (e) cloud OD; (f) Cloud lidar ratios retrieved by HU lidar from 22:00 on 23 August, 2011 to 04:00 on 24 August, 2011 (local time).

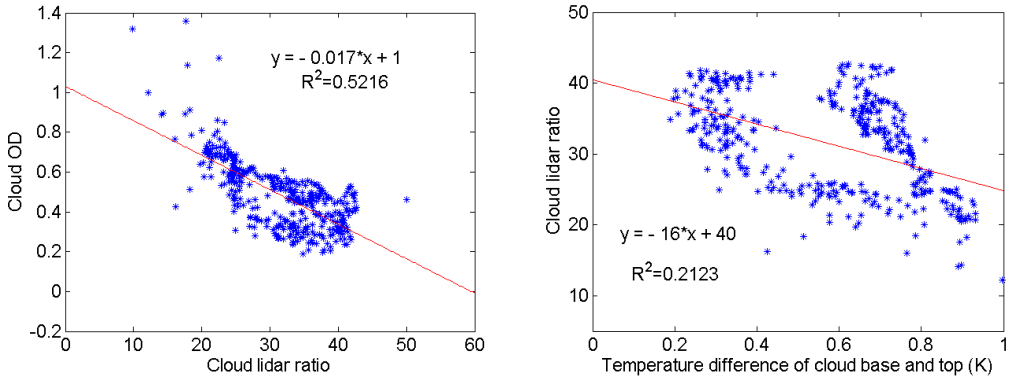

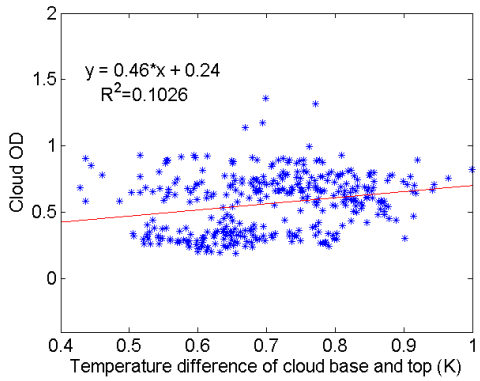

Fig.4 (a) Cloud OD as a function of cloud lidar ratios; (b) Cloud lidar ratios as a function of DCBT; (c) Cloud OD as a function of DCBT.

Acknowledgments

This study was supported by the National Oceanic and Atmospheric Administration (NOAA) under Grant - CREST Grant # NA06OAR4810162, and by the US Army Research, Development and Engineering Command (AQC) Center (DOD) under HU PIRT Award # 551150-211150).

References

Albrecht, B. A., Cox, S.K., & Schubert, W. H. (1979), Radiometric measurements of in-cloud temperature fluctuations. J. Appl. Meteor, 18, 1066-1068.

Ansmann, A., Riebesell, M., & Weitkamp, C. (1990), Measurement of atmospheric aerosol extinction profiles with a raman lidar. Opt. Lett., 15, 746-751.

Arshinov, Y. F., Bobrovnikov, S. M., Zuev, V. E., & Mitev, V. M. (1983), Atmospheric temperature measurements using a pure RR lidar. Appl. Opt., 22, 2984–2990.

Behrendt, A., & Reichardt, J. (2000), Atmospheric temperature profiling in the presence of clouds with a pure RR lidar by use of an interference-filter-based polychromator. Appl. Opt., 39, 1372-1376.

Brooks, I. M. (2003), Finding Boundary Layer Top: Application of a wavelet covariance transform to lidar backscatter profiles. J. Atmos. Ocean. Tech., 20, 1092–1105. DOI: http://dx.doi.org/10.1175/1520-0426(2003)020<1092:FBLTAO>2.0.CO;

Compton, J. C., Delgado, R., Berkoff, T. A., & Hoff, R. M. (2013), Determination of Planetary Boundary Layer Height on Short Spatial and Temporal Scales: A Demonstration of the Covariance Wavelet Transform in Ground-Based Wind Profiler and Lidar Measurements. J. Atmos. Ocean. Tech., 30, 1566–1575. DOI: http://dx.doi.org/10.1175/JTECH-D-12-00116.1;

Cooney, J., (1972), Measurement of atmospheric temperature profiles by Raman backscatter. J. Appl. Meteorol., 11, 108–112.

Davis, K. J., Gamage, N., Hagelberg, C. R., Kiemle, C., Lenschow, D. H. & Sullivan, P. P. (2000), An Objective Method for Deriving Atmospheric Structure from Airborne Lidar Observations. J. Atmos. Ocean. Tech., 17(11), 1455–1468. DOI: http://dx.doi.org/10.1175/1520-0426(2000)017;

Paleti, R., Kumar, Y.B., & Chaitanya, T.K. (2013), Wavelet transform method for deriving atmospheric boundary layer height from lidar. International Journal of Engineering and Technology, 5, 1465-1473.

Platnick, S., King, M. D. Ackerman, S. A., Menzel, W. P., Baum, B. A., Riédi, J. C., & Frey, R. A. (2003), The MODIS cloud products: Algorithms and examples from Terra. IEEE Trans. Geosci. Remote Sens., 41, 459–473.
Rossow, W.B., & Schiffer, R.A. (1999), Advances in understanding clouds from ISCCP. Bull. Amer. Meteorol. Soc., 80, 2261-2288. doi:10.1175/152-0477(1999)080<2261:AIUCFI>2.0.
Sinkevich, A. A., & Lawson, R. P. (2005), A Survey of Temperature Measurements in Convective Clouds. J. Appl. Meteor, 44, 1133-1136.
Solomon, S., D. Qin, M. Manning, Z. Chen, M. Marquis, K. B. Averyt, M. Tignor, & H. L. Miller, 2007: Climate Change 2007: The Physical Science Basis. Cambridge University Press, 996
Stokes, G. M., & Schwartz, S. E. (1994), The Atmospheric Radiation Measurement (ARM) Program: Programmatic background and design of the cloud and radiation testbed. Bull. Amer. Meteor. Soc., 75, 1201–1221.
Su, J., McCormick, M. P., Wu, Y., Lee III, R. B., Lei, L., Liu, Z., & Leavor, K. R. (2013), Cloud temperature measurement using rotational Raman lidar. Journal of Quantitative Spectroscopy & Radiative Transfer, 125, 45-50.
Su, J., McCormick, M. P., Liu, Z., Leavor, K., Lee III, R. B., Lewis, J., & Hill, M. T. (2010), Obtaining ground-based lidar geometrical form factors using coincident spaceborne lidar measurements. Appl. Opt., 49, 108-113.
Winker, D. M., Pelon, R. J., McCormick, M. P. (2003), The CALIPSO mission: spaceborne lidar for observation of aerosols and clouds. Proc. SPIE., 4893. doi: 10.1117/12.466539; http://dx.doi.org/10.1117/12.466539